

# Fast Ion Isotropization by Current Sheet Scattering in Magnetic Reconnection Jets

Louis Richard\*

*Swedish Institute of Space Physics, Uppsala, Sweden and  
Department of Physics and Astronomy, Space and Plasma Physics, Uppsala University, Sweden*

Yuri V. Khotyaintsev and Daniel B. Graham  
*Swedish Institute of Space Physics, Uppsala, Sweden*

Andris Vaivads  
*Space and Plasma Physics, School of Electrical Engineering,  
KTH Royal Institute of Technology, Stockholm, Sweden*

Daniel J. Gershman  
*NASA Goddard Space Flight Center, Greenbelt, Maryland 20771, USA*

Christopher T. Russell  
*University of California, Los Angeles, California 90095, USA*  
(Dated: February 2, 2023)

We present a statistical analysis of ion distributions in magnetic reconnection jets using data from the Magnetospheric Multiscale spacecraft. Compared with the quiet plasma in which the jet propagates, we often find anisotropic and non-Maxwellian ion distributions in the plasma jets. We observe magnetic field fluctuations associated with unstable ion distributions, but the wave amplitudes are not large enough to scatter ions during the observed lifetime of the jet. We estimate that the phase-space diffusion due to chaotic and quasi-adiabatic ion motion in the current sheet is sufficiently fast to be the primary process leading to isotropization.

Fast plasma flows, referred to as jets, are ubiquitous phenomena in the universe [1–3]. The dynamical evolution of the plasma jets is thought to be driven by changes in the magnetic field configuration (e.g., the Blandford-Znajek mechanism [4]). Magnetic reconnection, in particular, is a topological reconfiguration of the magnetic field, which results in the conversion of the magnetic field energy into particle energy through particle acceleration and heating [5, 6]. Complex non-Maxwellian ion velocity distribution functions (VDFs) characterize collisionless plasmas [7]. For example, cold Alfvénic counter-streaming ion beams entering into the reconnection exhaust [8, 9] provide a source of free energy for ion beam-driven instabilities [10]. Simulations [11, 12] have shown that as the beams cross the reconnection jet, heating of the beams results in the formation of a single VDF with parallel temperature anisotropy  $R_i = T_{i\perp}/T_{i\parallel} < 1$ , where  $T_{i\parallel}$  and  $T_{i\perp}$  are the ion temperature parallel and perpendicular to the magnetic field  $\mathbf{B}$ . Deviations from the thermal equilibrium drive micro-instabilities [13], contributing to ion heating in the reconnection region.

Spacecraft observations suggest waves grow in the reconnection jet due to ion-temperature-anisotropy instabilities [14, 15]. As the waves grow and saturate, pitch-angle scattering due to wave-particle interaction limits deviations from isotropy ( $T_{i\perp} = T_{i\parallel}$ ). Simulations indicate that the growth rate of the electromagnetic ion temperature anisotropy-driven instabilities is much slower than the driver of the unstable VDFs [12, 16]. As a result,

the unstable conditions persist for over hundreds of ion gyroperiods while being convected so that the unstable region of the jet can extend to hundreds  $d_i$  downstream of the reconnection site [12], with  $d_i = c/\omega_{pi}$  the ion inertial length. However, observations show a dominance of isotropic ion VDFs already at distances  $\sim 50 d_i$  from the reconnection region [15]. This disagreement between the simulations and observations suggests that other mechanisms relax the temperature anisotropy in the reconnection jets (e.g., betatron acceleration [17], Fermi acceleration [18], or current sheet pitch-angle scattering [19, 20]). Since, these mechanisms can efficiently heat the reconnection jet content, studying the processes limiting the ion temperature anisotropy is crucial to understanding the energy budget and partition in the reconnection jets.

In this Letter, we use data from the Magnetospheric Multiscale (MMS) spacecraft [21] in the Earth’s magnetotail to study the ion temperature anisotropy and non-Maxwellianity of ion VDFs in the reconnection jets. We show that the ion VDFs in the reconnection jets are efficiently isotropized on time scales much faster than provided by the wave-particle interactions.

We use 516 jets from a database of jets observed by MMS in the central plasma sheet (CPS) of the Earth’s magnetotail ( $\beta_i \geq 0.5$ , where  $\beta_i = n_i k_B T_i / P_{mag}$ ,  $n_i$  is the ion number density,  $T_i$  the ion temperature and  $P_{mag} = B^2/2\mu_0$  is the magnetic pressure) [22]. CPS plasma jets are thought to result from magnetic reconnection or kinetic ballooning/interchange instability [23]. It

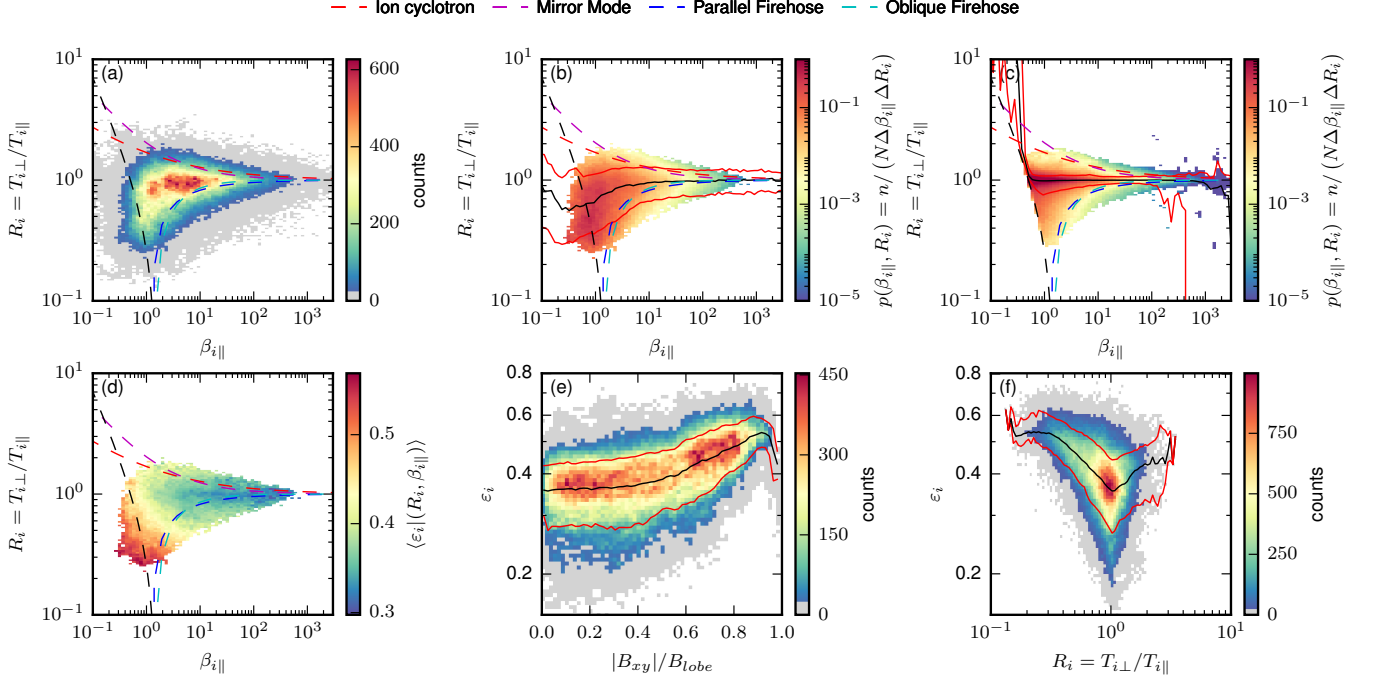


FIG. 1. Distribution of measurements. (a) Histogram of  $R_i = T_{i\perp}/T_{i\parallel}$  versus  $\beta_{i\parallel}$  in the reconnection jets. (b) and (c) distributions  $p(\beta_{i\parallel}, R_i)$  in the reconnection jets and quiet CPS ( $\beta_i > 0.5$ ,  $|V_i| < 100 \text{ km s}^{-1}$ ), respectively. The black line in panels (b)-(c) indicates the median of  $R_i$  as a function of  $\beta_{i\parallel}$ , and the red curves indicate the 10th and 90th percentiles. (d) Conditional average of  $\epsilon_i$  in the  $(\beta_{i\parallel}, R_i)$  space. The black dash line in panels (a)-(d) indicates the CPS threshold  $\beta_i \geq 0.5$ . (e) Histogram of  $\epsilon_i$  versus  $|B_{xy}|/B_{ext}$ . (f) Histogram of  $\epsilon_i$  versus  $n_i$ . The black line in panels (e)-(f) indicates the median of  $\epsilon_i$  as a function of  $|B_{xy}|/B_{ext}$  and  $R_i$  and the red curves indicate the 10th and 90th percentiles. Grey-shaded bins in panels (a), (e), and (f) indicate counts below  $5\sigma = 5\sqrt{n}$ .

is reasonable to assume that the plasma jets are primarily reconnection outflows since we observe the jets relatively close (the median distance is  $\delta x_c \approx 2.8 R_E$ ) to the statistical location of the reconnection X-line in the near-Earth magnetotail at  $X_{GSM} \approx -25 R_E$  in geocentric solar magnetospheric (GSM) coordinates [24]. The magnetic field is measured by the FGM instrument [25], and the ion VDFs are measured by the FPI-DIS instrument [26] with corrections removing a background population [27]. To increase the counting statistics and thus reduce the measurement uncertainties, we average the measurements across the four spacecraft and over a 450 ms (or three ion VDFs) running time window.

Overall, the ion VDFs are predominantly isotropic  $T_{i\perp} \sim T_{i\parallel}$  both in the reconnection jets [Fig. 1a and 1b] and in the quiet CPS [Fig. 1c]. However, compared to the quiet CPS, a significant fraction of the VDFs in the jets show a large deviation from  $T_{i\perp} = T_{i\parallel}$ , indicating that magnetic reconnection generates anisotropic VDFs.

Observations in the solar wind [28] have shown that the threshold  $\mathcal{R}_i$  for the ion temperature anisotropy driven instabilities scales with  $\beta_{i\parallel} = n_i k_B T_{i\parallel} / P_{mag}$  with:

$$\mathcal{R}_i = 1 + \frac{a}{(\beta_{i\parallel} - \beta_0)^b}, \quad (1)$$

where  $a$ ,  $b$ , and  $\beta_0$  are constants determined from linear Vlasov analysis of the kinetic dispersion relation in a homogeneous, magnetized, collisionless plasma with bi-Maxwellian ion VDFs [13]. Here we consider thresholds corresponding to the growth rate  $\gamma = 10^{-2} \omega_{ci}$  for a proton-electron plasma with isotropic electrons [29]. We observe that 70% of the ion VDFs lie within the instabilities thresholds, which might indicate that the temperature anisotropy is regulated in the reconnection jets by wave-particle interaction which we will investigate later.

Fig. 2 presents an example of a reconnection jet observed by MMS on August 21, 2017. The large amplitude oscillations of the magnetic field indicate the flapping of the magnetotail current sheet (CS) [30, 31]. The flapping enables sampling of the ion VDFs across the reconnection jet. We observe  $T_{i\parallel} > T_{i\perp}$  at the edges of the CS (maximum  $|\mathbf{B}|$ ) and  $T_{i\parallel} < T_{i\perp}$  at the CS center (minimum  $|\mathbf{B}|$ ) [Fig. 2c]. To investigate these large changes in temperature anisotropy, we compute the eigenvalues  $\lambda_1 > \lambda_2 > \lambda_3$  [Fig. 2d] and the eigenvectors of the temperature tensor [32]. At the CS edges, we observe  $\lambda_1/\lambda_2 > 1$  and  $\lambda_2/\lambda_3 \approx 1$  typical of two counter streaming beams VDFs while at the CS center, the anisotropy is reduced. We find that the eigenvectors are nearly constant throughout the interval with

$\hat{\mathbf{e}}_1 = [-0.99, 0.13, 0.03]$ , and  $\hat{\mathbf{e}}_3 = [-0.01, -0.28, 0.96]$  in GSM coordinates, and it is  $\mathbf{B}$  which rotates with respect to the constant eigenvectors [Fig. 2e] causing the large spikes in  $T_{i\perp}/T_{i\parallel}$ . Such behavior is consistent with the demagnetization of the ions in the CS center.

Fig. 2f shows the ion non-Maxwellianity  $\varepsilon_i = (2n_i)^{-1} \int |f_i - f_{i\text{bM}}| d^3v$  which is the normalized ( $\varepsilon_i \in [0, 1]$ ) zeroth-order moment of the difference between the observed ion VDF  $f_i$  and a bi-Maxwellian model  $f_{i\text{bM}}$  with the same moments [33]. The ion counting statistics are below the instrument noise floor at speeds  $v < v_{Ti}/3$  with  $v_{Ti} = \sqrt{2k_B T_i/m_i}$  due to the high ion bulk energy. For this reason, we compute  $\varepsilon_i$  using energy channels  $K_i > T_i/9$ . We see that  $\varepsilon_i$  changes significantly across the reconnection jet [Fig. 2f] and peaks at the CS edges. Simulations have shown that at the exhaust boundaries, the ion VDFs typically consist of cold Alfvénic counter-streaming beams [11, 12]. Such VDFs are non-velocity space-filling and thus yield a large  $\varepsilon_i$  consistent with our observations. In contrast,  $\varepsilon_i$  drops at the center of the CS, consistent with Speiser-like meandering ions filling the velocity space and resulting in a lower  $\varepsilon_i$ .

We observe that  $\varepsilon_i$ , which needs to be compared to the background value  $\varepsilon_i \approx 0.4$  in the quiet CPS, increases with decreasing  $\beta_{i\parallel}$  [Fig. 1d]. The same analysis repeated for a longer time averaging windows gives similar results. Fig. 1e presents  $\varepsilon_i$  as a function  $|\mathbf{B}_{xy}|/B_{ext}$ , which is a proxy of the distance to the CS center, and where  $B_{ext} = \sqrt{1 + \beta_i} |\mathbf{B}|$  is the external field obtained from pressure balance assumption. We observe that deviations from a bi-Maxwellian are statistically more pronounced at the CS edges, similar to that seen in Fig. 2f. In addition,  $\varepsilon_i$  and the temperature anisotropy are enhanced in the same regions [Fig. 1d and 1f], indicating that the magnetic reconnection drives both the temperature anisotropy and non-Maxwellianity.

The non-equilibrium VDFs can be unstable to a range of instabilities. To investigate this, we compute the magnetic field fluctuations  $|\delta\mathbf{B}|/B_0$  normalized to the background magnetic field  $B_0 = B_{ext}/2$  [30]. To remove the large-scale fluctuations, such as flapping, we high-pass filter  $\delta\mathbf{B}$  at  $f \geq 0.1$  Hz. Since the energy of the magnetic field fluctuations cascades to smaller scales, the power is dominated by the fluctuations at  $f \approx 0.1$  Hz, i.e.,  $k\rho_{i0} \approx 1.4 \pm 0.8$  where  $\rho_{i0} = v_{Ti}/\omega_{ci0}$  with  $\omega_{ci0} = eB_0/m_i$ . We observe strong magnetic wave activity in concert with the unstable ion VDFs [Fig. 3a] consistent with previous observations [14, 15]. This enhanced wave activity associated with unstable VDFs indicates the growth of the instabilities in the reconnection jets.

The majority of the observed ion VDFs are nearly isotropic  $T_{i\perp} \sim T_{i\parallel}$  [Fig. 1a], meaning that there must be a physical mechanism capable of reducing the anisotropy on time scales of the order of the jet lifetime. For this to be the ion kinetic instabilities, they first need

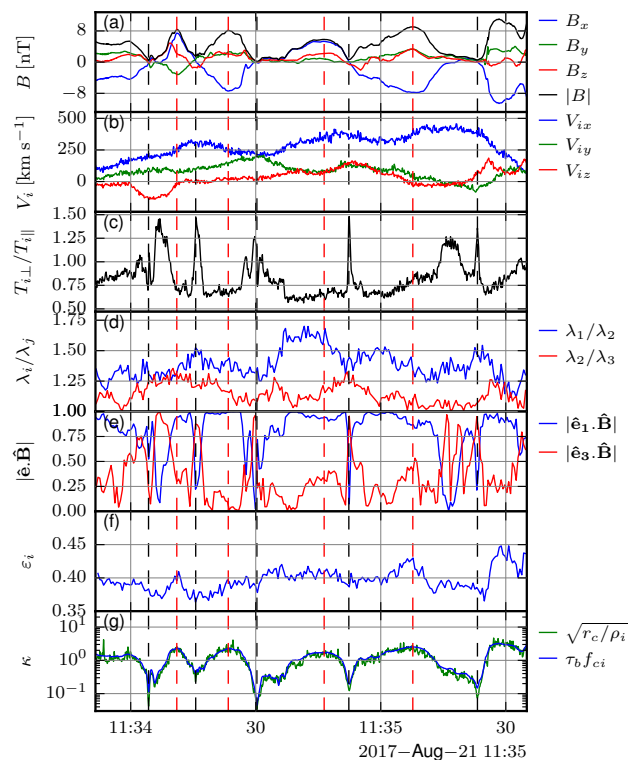


FIG. 2. Example reconnection jet with current sheet flapping motion. (a) Magnetic field. (b) Ion bulk velocity. (c) Ion temperature anisotropy  $T_{i\perp}/T_{i\parallel}$ , (d) ratios of the eigenvalues of the temperature tensor  $\mathbf{T}_i$  with  $\lambda_1 > \lambda_2 > \lambda_3$ . (e)  $\hat{\mathbf{e}}_1 \cdot \mathbf{B}$  and  $\hat{\mathbf{e}}_3 \cdot \mathbf{B}$  where  $\hat{\mathbf{e}}_1$  and  $\hat{\mathbf{e}}_3$  are the eigenvectors of  $\mathbf{T}_i$  associated with  $\lambda_1$  and  $\lambda_3$ . (f) Non-Maxwellianity  $\varepsilon_i$ . (g) Adiabaticity parameter  $\kappa$  from 4 spacecraft method  $\kappa = \sqrt{r_c/\rho_i}$  (green) and time scales ratio  $\kappa = \tau_b f_{ci}$  (blue).

to grow to large amplitudes and then have sufficient time to scatter the ions. We estimate the lifetime of the jet as  $\tau_c = \delta x/v_{A0}$  or  $\tau_c f_{ci0} = (2\pi)^{-1} \delta x/d_i$ , where  $f_{ci0} = \omega_{ci0}/2\pi$  and  $\delta x$  is the jet travel distance between the location of the spacecraft and the statistical location of the reconnection X-line at  $X_{GSM} = -25 R_E$  [24]. In the regions beyond the instabilities thresholds, we find  $\tau_c f_{ci0} \sim 10$ , and slightly higher values in the region bounded by the thresholds [Fig. 3b]. Thus, for the instability to grow to a sufficiently large amplitude, the growth rate needs to be very large,  $\gamma > 10^{-1} \omega_{ci}$ , which requires substantial temperature anisotropy [34]. There is a small fraction of points with anisotropies compatible with such high growth rates for  $T_{i\parallel} > T_{i\perp}$ , but none for  $T_{i\parallel} < T_{i\perp}$ , therefore it is unclear if the fluctuations can grow to sufficiently large amplitudes.

The pitch-angle scattering time  $\tau_s$  due to ion scale ( $k\rho_{i0} \sim 1$ ) Alfvénic fluctuations can be estimated as  $\tau_s f_{ci0} \sim (|\delta\mathbf{B}|/B_0)^{-2}$  [35, 36]. We find that the pitch-angle scattering time  $\tau_s$  is typically much larger than the jet lifetime  $\tau_c$  [Fig. 3c], indicating that the wave amplitudes are not sufficiently large to scatter ions over

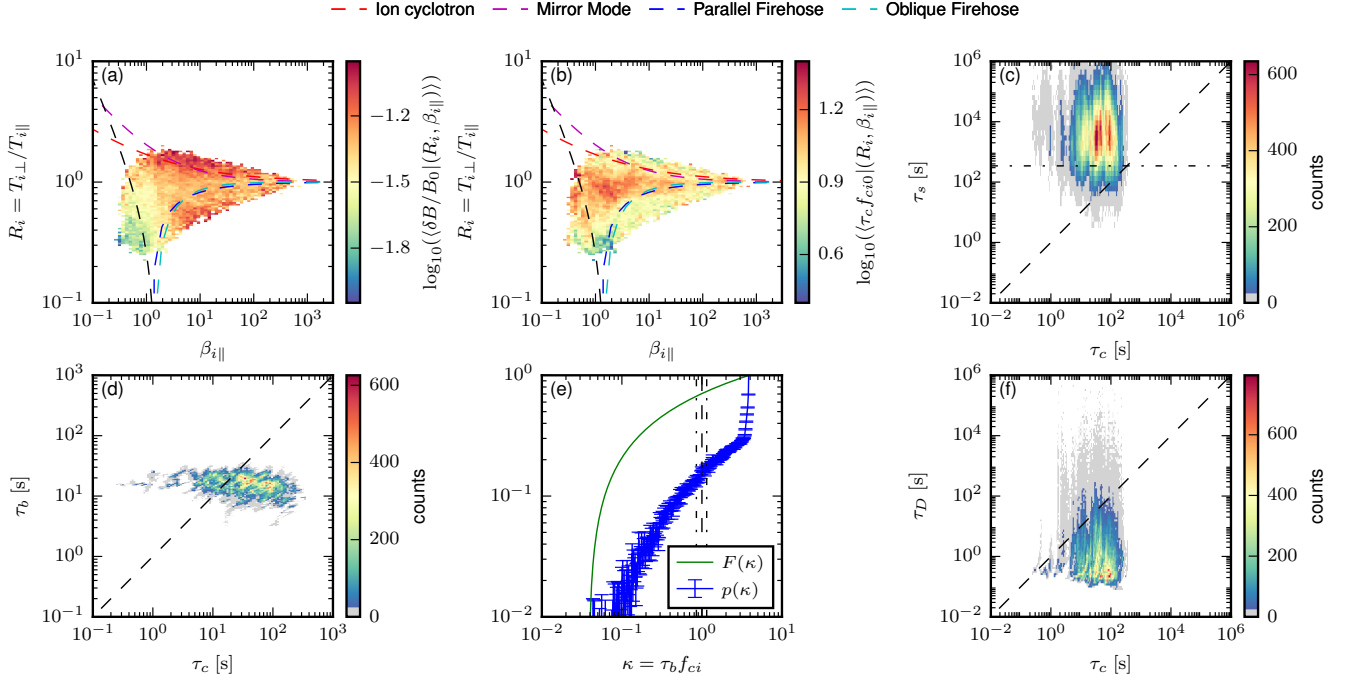


FIG. 3. Comparison of diffusion time scales and lifetime of the jet. (a) Magnetic field fluctuation normalized to the background field. (b) The lifetime of the jet. (c) Pitch-angle scattering time  $\tau_s$  due to Alfvénic fluctuations versus lifetime  $\tau_c$ . (d) Bouncing time  $\tau_b$  versus lifetime  $\tau_c$ . (e) Probability density function  $p$  and cumulative distribution function  $F$  of  $\kappa = \tau_b f_{ci}$ . (f) Phase-space diffusion time  $\tau_D$  versus lifetime  $\tau_c$ .

the lifetime of the jet. In particular, the time required for waves to scatter ions is  $\tau_c f_{ci0} \sim \tau_s f_{ci0}$  and during that time, the jet would travel a distance  $\delta x \sim 2\pi(|\delta \mathbf{B}|/B_0)^{-2} d_i \sim 2\pi \times 10^3 d_i \approx 400 R_E$  which is much larger than the distance from reconnection region to spacecraft  $\delta x_c \approx 2.8 R_E$ . This suggests that another more efficient isotropization mechanism is at play.

Ion VDFs are close to isotropic, and  $\varepsilon_i$  is minimum at the CS center [Fig. 2] suggesting efficient scattering in highly curved magnetic fields ( $r_c \ll \rho_i$  where  $r_c = |\mathbf{b} \cdot \nabla \mathbf{b}|^{-1}$  is the magnetic field curvature radius with  $\mathbf{b} = \mathbf{B}/|\mathbf{B}|$ ). The ion motion in the CS can be described in terms of competition between bouncing motion across the CS and gyromotion in the CS around a finite normal magnetic field  $B_n$  [37, 38]. The ratio of bouncing and gyromotion time scales is given by  $\kappa = \tau_b f_{ci}$  [20], where  $\tau_b = 2\pi/\omega_b = 2\pi/\sqrt{v_0 \omega_{ci0}}/L$  with  $v_0$  the characteristic particle velocity and  $L \approx 20\rho_i$  the average CS thickness from statistical studies [39]. Since we observe  $T_{i\parallel} \gg T_{i\perp}$  at the CS edges, we assume that the ion population entering and escaping from the CS consist of two cold Alfvénic counter streaming ion beams [8] so that  $v_0 = v_{A0}$ . Alternatively,  $\kappa$  can be defined as the curvature parameter  $\kappa = \sqrt{r_c}/\rho_i$  [20], which can be estimated using multi-spacecraft methods [40, 41]. We find an excellent agreement between the two estimates [Fig. 2g] indicating that the assumptions of  $v_0 = v_{A0}$  and  $L \approx 20\rho_i$  are reasonable.

The ion motion is adiabatic with the magnetic moment  $\mu = mv_{\perp}^2/2B$  conserved when the gyromotion is faster than the bouncing motion  $\kappa \gg 1$ . For  $\kappa \sim 1$ , the ion motion becomes stochastic [20]. For  $\kappa \ll 1$ , the ion motion is quasi-adiabatic with the generalized magnetic moment  $I_z = (2\pi)^{-1} \int p_z dz$  as an integral of motion, where  $(z, p_z)$  are the variables of the fast bouncing motion [20]. We observe in Fig. 2g that  $\kappa \leq 1$  near the CS center, meaning that the ions are in the chaotic and quasi-adiabatic regime in a thin  $l \approx \rho_i$  [42] layer in the vicinity of the CS center consistent with the observed demagnetization of the ions in the CS center. From Fig. 3e we see that 73% of the ion VDFs are in the chaotic and quasi-adiabatic motion regime ( $F(\kappa = 1) = 0.73$ ). We expect strong pitch-angle scattering in the CS in these regimes, which reduces the anisotropy [19, 20].

The pitch-angle scattering in the CS is related to the destruction of  $I_z$  for particles in the chaotic and quasi-adiabatic motion regime ( $\kappa \lesssim 1$ ). Studies of the Hamiltonian of the ion motion in the CS showed that the characteristic phase-space diffusion time is  $\tau_D f_{ci0} \sim \kappa^{-3}$  [20, 38]. As the solution of the diffusion equation is exponentially decaying in time, the steady (99%) state isotropic VDF is reached after  $t = 2 \log(10)\tau_D$ . Since the effective ion pitch-angle scattering occurs in the thin ( $l \approx \rho_i \approx L/20$ ) layer where  $\kappa \leq 1$  [42], the diffusion time is increased by a factor of 20 compared to scattering in the entire thick CS. These yield the effective diffusion

time  $\tau_{eff} \approx 40 \log(10) \tau_D \sim 100 \tau_D$ . From Fig. 1f, we find that  $\tau_D \sim 0.01 \tau_c$ , so that the effective diffusion time is similar to the lifetime of the observed jets,  $\tau_c \approx \tau_{eff}$ . In particular, we find that the effective characteristic scattering time is  $\tau_{eff} \approx 18 \text{ s} \approx 3.3 f_{ci0}^{-1}$ . It follows that the travel distance from the X-line necessary to scatter the ions is  $\delta x \sim 2\pi \times 3.3 d_i \approx 20 d_i \approx 1.5 R_E < \delta x_c \approx 2.8 R_E$ . This indicates that the interaction with the CS can efficiently scatter ions during the observed lifetime of the jets.

We have presented a statistical investigation of the ion VDFs in reconnection jets. Our results show that overall the observed ion VDFs are isotropic but are often driven out of thermal equilibrium by magnetic reconnection. These unstable VDFs excite micro-instabilities resulting in enhanced wave activity. From quasi-linear theory [43], the instabilities can grow to large amplitudes after  $10 - 100 f_{ci0}^{-1}$  consistent with our observation. Then, wave-particle interaction can isotropize ion VDFs after  $\sim 10^3 f_{ci0}^{-1}$ . However, this implies that during this time, the jets would need to travel a distance  $\delta x \sim 2\pi \times 10^3 d_i$ , which is much larger than the observed distance to the X-line, meaning that wave-particle scattering is not sufficiently fast to explain the predominantly isotropic ion VDFs within the observed jets. The situation may be different in denser environments where the wave-particle interaction can scatter ions over shorter distances compared with the system size (e.g., for coronal loops  $n_i \sim 1 \times 10^{15} \text{ m}^{-3}$  [44],  $\delta x \sim 45 \text{ km}$ ).

We find that the phase-space diffusion due to chaotic and quasi-adiabatic ion motion in the CS is sufficiently fast to be the primary process leading to isotropization. In particular, we find that the travel distance needed to scatter ions is  $\delta x \approx 20 d_i$  consistent with nearly isotropic ion VDFs observed at distances  $> 10 d_i$  from the reconnection X-line in simulations [45, 46]. Studies of the Hamiltonian of the ion motion [47, 48] have shown that in the presence of a guide-field such as at astrophysical plasma jets, the phase-space diffusion is faster suggesting that for these environments the regulation of the ion anisotropy may be very efficient.

MMS data are available at the MMS Science Data Center; see Ref. [49]. Data analysis was performed using the `pyrfu` analysis package [50].

We thank the MMS team and instrument PIs for data access and support. This work is supported by the Swedish National Space Agency Grant 139/18.

---

\* louis.richard@irfu.se

- [1] S. Masuda, T. Kosugi, H. Hara, S. Tsuneta, and Y. Ogawara, *Nature* **371**, 495 (1994).  
 [2] T. D. Phan, L. M. Kistler, B. Klecker, G. Haerendel, G. Paschmann, B. U. Ö. Sonnerup, W. Baumjohann, M. B. Bavassano-Cattaneo, C. W. Carlson, A. M.

- DiLellis, K.-H. Fornaçon, L. A. Frank, M. Fujimoto, E. Georgescu, S. Kokubun, E. Moebius, T. Mukai, M. Øieroset, W. R. Paterson, and H. Reme, *Nature* **404**, 848 (2000).  
 [3] R. E. Pudritz, M. J. Hardcastle, and D. C. Gabuzda, *Space Science Reviews* **169**, 27 (2012).  
 [4] K. Parfrey, A. Philippov, and B. Cerutti, *Physical Review Letters* **122**, 035101 (2019).  
 [5] D. Biskamp, *Magnetic reconnection in plasmas*, Cambridge Monographs on Plasma Physics (Cambridge University Press, Cambridge, 2000).  
 [6] M. Yamada, R. Kulsrud, and H. Ji, *Reviews of Modern Physics* **82**, 603 (2010).  
 [7] M. Hoshino, T. Mukai, T. Yamamoto, and S. Kokubun, *Journal of Geophysical Research: Space Physics* **103**, 4509 (1998).  
 [8] T. Nagai, M. Nakamura, I. Shinohara, M. Fujimoto, Y. Saito, and T. Mukai, *Physics of Plasmas* **9**, 3705 (2002).  
 [9] J. P. Eastwood, M. V. Goldman, H. Hietala, D. L. Newman, R. Mistry, and G. Lapenta, *Journal of Geophysical Research: Space Physics* **120**, 511 (2015).  
 [10] C. M. Liu, A. Vaivads, D. B. Graham, Y. V. Khotyaintsev, H. S. Fu, A. Johlander, M. André, and B. L. Giles, *Geophysical Research Letters* **46**, 12702 (2019).  
 [11] J. F. Drake, M. Swisdak, T. D. Phan, P. A. Cassak, M. A. Shay, S. T. Lepri, R. P. Lin, E. Quataert, and T. H. Zurbuchen, *Journal of Geophysical Research: Space Physics* **114**, A05111 (2009).  
 [12] H. Hietala, J. F. Drake, T. D. Phan, J. P. Eastwood, and J. P. McFadden, *Geophysical Research Letters* **42**, 7239 (2015).  
 [13] S. P. Gary, *Theory of space plasma microinstabilities*, Cambridge atmospheric and space science series (Cambridge University Press, Cambridge, 1993).  
 [14] Z. Vörös, *Nonlinear Processes in Geophysics* **18**, 861 (2011).  
 [15] M. Wu, M. Volwerk, Q. Lu, Z. Vörös, R. Nakamura, and T. Zhang, *Journal of Geophysical Research: Space Physics* **118**, 4875 (2013).  
 [16] M. W. Kunz, A. A. Schekochihin, and J. M. Stone, *Physical Review Letters* **112**, 205003 (2014).  
 [17] X. Zhou, Y. Xu, A. Runov, J. Liu, A. V. Artemyev, V. Angelopoulos, J. Birn, Z. Yao, D. Pan, and Q. Zong, *Journal of Geophysical Research: Space Physics* **124**, 4009 (2019).  
 [18] S. Lu, V. Angelopoulos, and H. Fu, *Journal of Geophysical Research: Space Physics* **121**, 9483 (2016).  
 [19] T. J. Birmingham, *Journal of Geophysical Research* **89**, 2699 (1984).  
 [20] J. Büchner and L. M. Zelenyi, *Journal of Geophysical Research* **94**, 11821 (1989).  
 [21] J. L. Burch, T. E. Moore, R. B. Torbert, and B. L. Giles, *Space Science Reviews* **199**, 5 (2016).  
 [22] L. Richard, Y. V. Khotyaintsev, D. B. Graham, and C. T. Russell, *Geophysical Research Letters* **49**, 10.1029/2022GL101693 (2022).  
 [23] P. L. Pritchett and F. V. Coroniti, *Journal of Geophysical Research: Space Physics* **115**, 10.1029/2009JA014752 (2010).  
 [24] T. Nagai, M. Fujimoto, R. Nakamura, W. Baumjohann, A. Ieda, I. Shinohara, S. Machida, Y. Saito, and T. Mukai, *Journal of Geophysical Research: Space Physics* **110**, 10.1029/2005JA011207 (2005).

- [25] C. T. Russell, B. J. Anderson, W. Baumjohann, K. R. Bromund, D. Dearborn, D. Fischer, G. Le, H. K. Leinweber, D. Leneman, W. Magnes, J. D. Means, M. B. Moldwin, R. Nakamura, D. Pierce, F. Plaschke, K. M. Rowe, J. A. Slavin, R. J. Strangeway, R. Torbert, C. Hagen, I. Jernej, A. Valavanoglou, and I. Richter, *Space Science Reviews* **199**, 189 (2016).
- [26] C. Pollock, T. Moore, A. Jacques, J. Burch, U. Gliese, Y. Saito, T. Omoto, L. Avanov, A. Barrie, V. Coffey, J. Dorelli, D. Gershman, B. Giles, T. Rosnack, C. Salo, S. Yokota, M. Adrian, C. Aoustin, C. Auletta, S. Aung, V. Bigio, N. Cao, M. Chandler, D. Chornay, K. Christian, G. Clark, G. Collinson, T. Corris, A. De Los Santos, R. Devlin, T. Diaz, T. Dickerson, C. Dickson, A. Diekmann, F. Diggs, C. Duncan, A. Figueroa-Vinas, C. Firman, M. Freeman, N. Galassi, K. Garcia, G. Goodhart, D. Guerero, J. Hageman, J. Hanley, E. Hemminger, M. Holland, M. Hutchins, T. James, W. Jones, S. Kreisler, J. Kujawski, V. Lavu, J. Lobell, E. LeCompte, A. Lukemire, E. MacDonald, A. Mariano, T. Mukai, K. Narayanan, Q. Nguyen, M. Onizuka, W. Paterson, S. Persyn, B. Piepgrass, F. Cheney, A. Rager, T. Raghuram, A. Ramil, L. Reichenthal, H. Rodriguez, J. Rouzaud, A. Rucker, Y. Saito, M. Samara, J.-A. Sauvaud, D. Schuster, M. Shappirio, K. Shelton, D. Sher, D. Smith, K. Smith, S. Smith, D. Steinfeld, R. Szymkiewicz, K. Tanimoto, J. Taylor, C. Tucker, K. Tull, A. Uhl, J. Vloet, P. Walpole, S. Weidner, D. White, G. Winkert, P.-S. Yeh, and M. Zeuch, *Space Science Reviews* **199**, 331 (2016).
- [27] D. J. Gershman, J. C. Dorelli, L. A. Avanov, U. Gliese, A. Barrie, C. Schiff, D. E. Da Silva, W. R. Paterson, B. L. Giles, and C. J. Pollock, *Journal of Geophysical Research: Space Physics* **124**, 10345 (2019).
- [28] P. Hellinger, P. Trávníček, J. C. Kasper, and A. J. Lazarus, *Geophysical Research Letters* **33**, L09101 (2006).
- [29] D. Verscharen, B. D. G. Chandran, K. G. Klein, and E. Quataert, *The Astrophysical Journal* **831**, 128 (2016).
- [30] V. A. Sergeev, A. Runov, W. Baumjohann, R. Nakamura, T. L. Zhang, M. Volwerk, A. Balogh, H. Rème, J. A. Sauvaud, M. André, and B. Klecker, *Geophysical Research Letters* **30**, 10.1029/2002GL016500 (2003).
- [31] L. Richard, Y. V. Khotyaintsev, D. B. Graham, M. I. Sitnov, O. Le Contel, and P. Lindqvist, *Journal of Geophysical Research: Space Physics* **126**, 10.1029/2021JA029152 (2021).
- [32] S. Servidio, F. Valentini, F. Califano, and P. Veltri, *Physical Review Letters* **108**, 045001 (2012).
- [33] D. B. Graham, Y. V. Khotyaintsev, M. André, A. Vaivads, A. Chasapis, W. H. Matthaeus, A. Retinò, F. Valentini, and D. J. Gershman, *Journal of Geophysical Research: Space Physics* **126**, 10.1029/2021JA029260 (2021).
- [34] B. A. Maruca, A. Chasapis, S. P. Gary, R. Bandyopadhyay, R. Chhiber, T. N. Parashar, W. H. Matthaeus, M. A. Shay, J. L. Burch, T. E. Moore, C. J. Pollock, B. J. Giles, W. R. Paterson, J. Dorelli, D. J. Gershman, R. B. Torbert, C. T. Russell, and R. J. Strangeway, *The Astrophysical Journal* **866**, 25 (2018).
- [35] S. D. Bale, J. C. Kasper, G. G. Howes, E. Quataert, C. Salem, and D. Sundkvist, *Physical Review Letters* **103**, 211101 (2009).
- [36] C. F. Kennel and H. E. Petschek, *Journal of Geophysical Research* **71**, 1 (1966).
- [37] J. Chen, *Journal of Geophysical Research* **97**, 15011 (1992).
- [38] L. M. Zelenyi, A. I. Neishtadt, A. V. Artemyev, D. L. Vainchtein, and H. V. Malova, *Physics Uspekhi* **56**, 347 (2013).
- [39] A. Runov, V. A. Sergeev, W. Baumjohann, R. Nakamura, S. Apatenkov, Y. Asano, M. Volwerk, Z. Vörös, T. L. Zhang, A. Petrukovich, A. Balogh, J.-A. Sauvaud, B. Klecker, and H. Rème, *Annales Geophysicae* **23**, 1391 (2005).
- [40] G. Chanteur, *ISSI Scientific Reports* , 349 (1998).
- [41] G. Chanteur and C. C. Harvey, *ISSI Scientific Reports* , 371 (1998).
- [42] A. V. Artemyev, A. A. Petrukovich, R. Nakamura, and L. M. Zelenyi, *Journal of Geophysical Research: Space Physics* **115**, 10.1029/2010JA015702 (2010).
- [43] P. H. Yoon, *Reviews of Modern Plasma Physics* **1**, 4 (2017).
- [44] F. Reale, *Living Reviews in Solar Physics* **11**, 10.12942/lrsp-2014-4 (2014).
- [45] N. Aunai, G. Belmont, and R. Smets, *Journal of Geophysical Research: Space Physics* **116**, 10.1029/2011JA016688 (2011).
- [46] A. Divin, Y. V. Khotyaintsev, A. Vaivads, M. André, S. Toledo-Redondo, S. Markidis, and G. Lapenta, *Journal of Geophysical Research: Space Physics* **121**, 12,001 (2016).
- [47] A. V. Artemyev, A. I. Neishtadt, and L. M. Zelenyi, *Physical Review E* **89**, 060902 (2014).
- [48] A. V. Artemyev, A. I. Neishtadt, A. A. Vasiliev, V. Angelopoulos, A. A. Vinogradov, and L. M. Zelenyi, *Physical Review E* **102**, 033201 (2020).
- [49] See <https://lasp.colorado.edu/mms/sdc/public>.
- [50] See <https://pypi.org/project/pyrfu/>.